

Multimodal Machine Learning for Soft High- k Elastomers under Data Scarcity

Brijesh FNU,[†] Viet Thanh Duy Nguyen,[‡] Ashima Sharma,[†] Md Harun Rashid Molla,[†] Chengyi Xu,^{*,†} and Truong-Son Hy^{*,‡}

[†]*Department of Mechanical and Materials Engineering, School of Engineering, The University of Alabama at Birmingham (UAB)*

[‡]*Department of Computer Science, College of Arts and Sciences, The University of Alabama at Birmingham (UAB)*

E-mail: cxu@uab.edu; thy@uab.edu

Abstract

Dielectric materials are critical building blocks for modern electronics such as sensors, actuators, and transistors. With the rapid recent advance in soft and stretchable electronics for emerging human- and robot-interfacing applications, there is a surging need for high-performance dielectric elastomers. However, it remains a grand challenge to develop soft elastomers that simultaneously possess high dielectric constants (k , related to energy storage capacity) and low Young's moduli (E , related to mechanical flexibility). While some new elastomer designs have been reported in individual (mostly one-off) studies, almost no structured dataset is currently available for dielectric elastomers that systematically encompasses their molecular sequence, dielectric, and mechanical properties. Within this context, we curate a compact, high-quality dataset of acrylate-based dielectric elastomers, one of the most widely explored elastomer backbones due to its versatile chemistry and molecular design flexibility, by screening and aggregating experimental results from the literature over the past 10 years.

Building on this dataset, we propose a multimodal learning framework that leverages large-scale pretrained polymer representations from graph- and sequence-based encoders. These pretrained embeddings transfer rich chemical and structural knowledge from vast polymer corpora, enabling accurate few-shot prediction of both dielectric and mechanical properties from molecular sequences. Our results represent a new paradigm for transferring knowledge from pretrained multimodal models to overcome severe data scarcity, which can be readily translated to other polymer backbones (e.g., silicones, urethanes) and thus accelerate data-efficient discovery of soft high- k dielectric elastomers. Our source code and dataset are publicly available at <https://github.com/HySonLab/Polymers>.

1 Introduction

Soft and stretchable electronics underpin emerging human- and robot-interfacing technologies such as wearable and implantable sensors, artificial muscles, and epidermal transistors. Among these, polymers that simultaneously exhibit a high dielectric constant (k , related to energy storage capacity) and a low Young’s modulus (E , related to mechanical flexibility) are particularly sought after, as they enable strong electromechanical coupling and high energy density while preserving mechanical compliance. Yet, achieving this balance remains a grand challenge in polymer science. Inorganic dielectrics typically offer excellent dielectric constants but are rigid and brittle, whereas organic polymers provide flexibility at the cost of low dielectric performance. Reconciling these opposing characteristics within a single material, therefore, requires a delicate molecular design trade-off.

Recently, machine learning (ML) has emerged as a promising paradigm to accelerate materials discovery by uncovering structure-property relationships directly from data.^{1,2} ML models can capture complex, nonlinear correlations between polymer structure and functional properties, enabling rapid virtual screening and guiding targeted synthesis. However, the effectiveness of ML-driven materials design hinges on the availability of high-quality datasets with consistent and well-annotated measurements.

In the context of soft dielectric elastomers, dielectric constants and mechanical properties such as Young’s modulus are often reported separately across individual studies, making it challenging to directly leverage these measurements for integrated data-driven modeling. The lack of a unified, machine-readable dataset that jointly organizes dielectric and mechanical information motivates the need for careful data curation and standardized benchmarking. Addressing this challenge is essential for developing data-efficient learning frameworks capable of operating under realistic, data-scarce conditions.

In this work, we curate a compact, well-structured dataset of acrylate-based polymers, as acrylates are one of the most widely explored elastomer backbones due to their versatile compatible chemistries and exceptional molecular design flexibility, by aggregating experimentally reported dielectric constants and Young’s moduli from the literature. Each entry was manually verified and standardized to ensure consistency and reproducibility, providing a reliable foundation for data-driven modeling of soft high- k dielectric elastomers under extreme data scarcity. Furthermore, to effectively learn from such limited data, we introduce a multimodal, data-efficient learning framework that leverages large-scale pretrained polymer representations. By integrating complementary embeddings from pretrained graph- and sequence-based encoders, the framework transfers rich chemical and structural knowledge acquired from vast polymer corpora to this small, specialized domain. This transfer enables robust few-shot learning of structure-property relationships, yielding accurate predictions of both dielectric and mechanical behavior. Together, the curated dataset and pretrained multimodal framework establish a foundation for accelerating the discovery of soft high- k dielectric elastomers under data-limited conditions.

2 Related Work

2.1 Polymer Property Prediction

Polymer property prediction is a central challenge in polymer informatics, where machine learning and deep learning methods have become powerful tools for uncovering structure-property re-

relationships.^{1,2} Early studies primarily employed classical algorithms such as multiple linear regression^{3,4} and kernel-based support vector machines⁵ to correlate polymer sequences with their measured properties. More recently, deep learning approaches have been introduced to capture the nonlinear and hierarchical dependencies within polymer structures. Convolutional neural networks (CNNs) have been applied to predict the mechanical behavior of polymer-carbon nanotube composites,⁶ while recurrent neural networks (RNNs) have been used to model sequential dependencies in polymer chains and their influence on physical or mechanical properties.^{7,8} Despite these advances, the predictive performance of data-driven models remains limited by the scarcity of large, high-quality polymer property datasets, a long-standing bottleneck in polymer informatics.

2.2 Pretrained Polymer Representations

Inspired by the remarkable success of pretrained language models in natural language processing (NLP), recent efforts in polymer informatics have explored Transformer-based pretraining to learn general-purpose polymer representations. These models treat polymer sequences or structural notations (such as SMILES,⁹ SMARTS¹⁰ or SELFIES¹¹) as textual data, enabling the application of self-supervised learning techniques originally developed for language understanding. By training on large, unlabeled polymer corpora, pretrained models can capture the underlying chemical syntax and structural regularities of polymer chains, producing embeddings that encode rich physicochemical and topological information. Several polymer language models, such as PolyBERT¹² and TransPolymer,¹³ have demonstrated strong performance across diverse downstream tasks, highlighting the potential of pretrained representations to enhance polymer property prediction and design under data-scarce conditions.

Recent studies have explored multimodal representation learning approaches that integrate textual descriptions, sequence-based representations, and three-dimensional (3D) structural modalities of polymers. By combining semantic information from text with molecular connectivity and spatial conformation, these multimodal frameworks have shown promising improvements in cap-

turing the complex structure-property relationships essential for accurate polymer modeling and design.^{14,15}

3 Dataset Curation

3.1 Data Sources

Experimental characterization of the dielectric and mechanical properties of soft dielectric elastomers is both costly and time-consuming, resulting in limited availability of such data in the public domain. Although numerous studies have reported k and E for individual polymer systems, these measurements are scattered across the literature and lack a unified, machine-readable format suitable for data-driven modeling. To address this limitation, we systematically collected and consolidated reported data from peer-reviewed publications on acrylate-based dielectric elastomers.^{16–40} In this study, we mainly focus on acrylates because they represent one of the most widely explored polymer backbones for dielectric elastomers due to their versatile chemistries and molecular design flexibility, and the same learning framework should be readily translatable to elastomers with alternative backbone motifs (e.g., silicones and urethanes) in subsequent studies.

From each source, we extracted three key quantities: the dielectric constant, Young's modulus, and the complete elastomer matrix formulation. Based on the reported chemical compositions, the corresponding repeat-unit structures were identified using the PubChem database and converted into SMILES representations to establish a consistent link between polymer structure and experimentally measured properties. In addition, each data record in the curated dataset includes the hyperlink to its original experimental source, ensuring full traceability and transparency. This curated dataset provides a reliable and standardized foundation for developing and benchmarking multimodal machine-learning models in soft high- k dielectric elastomer discovery.

3.2 Dataset Fields and Property Definitions

Each entry in the curated dataset corresponds to a unique acrylate-based dielectric elastomer formulation collected from the literature. For transparency and usability, every record includes experimentally measured properties together with structured representations of the polymer chemistry. The dataset fields and their physical meanings are summarized below:

1. **Dielectric Constant (k).** The dielectric constant quantifies the ability of an elastomer to store electrical energy when subjected to an external electric field. Higher k values indicate stronger polarization mechanisms and are directly associated with improved performance in applications such as capacitive sensors, dielectric elastomer actuators, and soft transducers. In the curated dataset, reported k values range from moderate permittivity elastomers ($k < 20$) to a small number of high- k systems ($k > 100$), reflecting diverse chemical strategies for enhancing dipolar polarization.
2. **Young's Modulus (E , MPa).** Young's modulus characterizes the mechanical stiffness of the elastomer and is typically extracted from the linear elastic region of tensile stress-strain measurements. Low modulus values correspond to mechanically soft and highly stretchable materials, which are essential for maintaining compliance in soft and wearable electronic devices. Most elastomers in the dataset exhibit sub-megapascal moduli, consistent with their intended use in soft electromechanical systems.
3. **SMILES Representation.** To enable computational modeling, each elastomer formulation is mapped to a simplified repeat-unit structure encoded as a SMILES string. This standardized, machine-readable representation describes the polymer backbone and functional groups and serves as the primary input for both sequence-based and graph-based learning models.
4. **Source Reference.** Each dataset entry includes a direct hyperlink to the original peer-reviewed publication from which the experimental measurements were extracted. This ensures full traceability and allows users to examine experimental conditions, synthesis protocols, and measurement methodologies in detail.

To illustrate the structure of the dataset, representative examples of elastomer entries are shown in Table 1. Together, these fields provide a comprehensive and interpretable representation of soft dielectric elastomers, enabling reproducible data-driven modeling and analysis.

Table 1: Representative examples from the curated soft dielectric elastomer dataset.

k	E (MPa)	SMILES Representation	Source Reference
168.0	5.3	<chem>*C(*)(C)C(=O)OCCCC.*c1ccc(N)c(N)c1*</chem>	https://www.sciencedirect.com/science/article/pii/S1359836819308303
96.1	4.52	<chem>[*]C(C)(C(=O)OCCCC)[*].[*]c1ccc([*])c([*])c1</chem>	https://dataset-dl.liris.cnrs.fr/db_amethyst/PDFs/10.1016/j.eurpolymj.2021.110418.pdf
5.2	0.24	<chem>[*]C(C)(C(=O)O[Ca]O(=O)C(C)[*]</chem>	https://www.sciencedirect.com/science/article/pii/S0032386117312430

3.3 Data Processing

Each data record underwent systematic processing to ensure structural consistency, reproducibility, and compatibility with subsequent machine-learning analyses. The key steps in this pipeline are summarized as follows:

1. **Unit Harmonization.** All dielectric constants (k) were treated as dimensionless quantities, and all Young's modulus (E) values were converted to megapascals (MPa), with dielectric constants restricted to values measured in the kHz frequency range.. This harmonization ensured that both electrical and mechanical properties were expressed in consistent SI units across all samples.
2. **Data Cleaning.** Records containing incomplete, ambiguous, or non-numeric property values were excluded. When multiple sources reported measurements for the same elastomer

formulation, mean property values were retained after discarding clear outliers to minimize experimental bias.

3. **Handling Missing Values.** Only elastomer samples with both dielectric constant and Young's modulus measurements were included in the final dataset. No synthetic imputation or estimation was applied in order to preserve the integrity of experimentally reported data.
4. **SMILES Extraction and Standardization.** Polymer matrix compositions obtained from the literature were converted into SMILES representations using the PubChem database. Each SMILES string was manually verified and standardized to ensure accurate parsing within RDKit for subsequent molecular feature generation.

This multi-stage data processing workflow ensured that every acrylate-based dielectric elastomer sample was represented in a chemically consistent and computationally reliable format, establishing a robust foundation for the downstream multimodal learning framework. To further support reproducibility and enable future research, we also provide precomputed molecular feature representations for each data sample, including Morgan fingerprints, PolyBERT and TransPolymer embeddings, and graph-based embeddings derived from our pretrained GNN encoder.

3.4 Dataset Statistics

After cleaning and standardization, the dataset contains a total of **35** unique acrylate-based dielectric elastomer entries, each with complete measurements of dielectric constant (k) and Young's modulus (E). The relatively small size of the dataset reflects the scarcity of jointly reported dielectric-mechanical measurements in the literature and underscores the importance of developing data-efficient learning approaches.

As illustrated in Figure 1, approximately 71% of acrylate-based dielectric elastomer in the dataset exhibit moderate dielectric constants ($k < 20$), with only a few high- k outliers exceeding 100. This trend suggests that strong polarization enhancement is relatively uncommon among soft dielectric materials. In contrast, Young's modulus (E) values are largely concentrated below 1 MPa, reflecting the predominance of ultra-softmechanically compliant elastomers suitable for

soft and stretchable electronics. Together, these distributions highlight the intrinsic trade-off between high dielectric constant and low modulus, underscoring the need for predictive modeling frameworks capable of learning from limited experimental data.

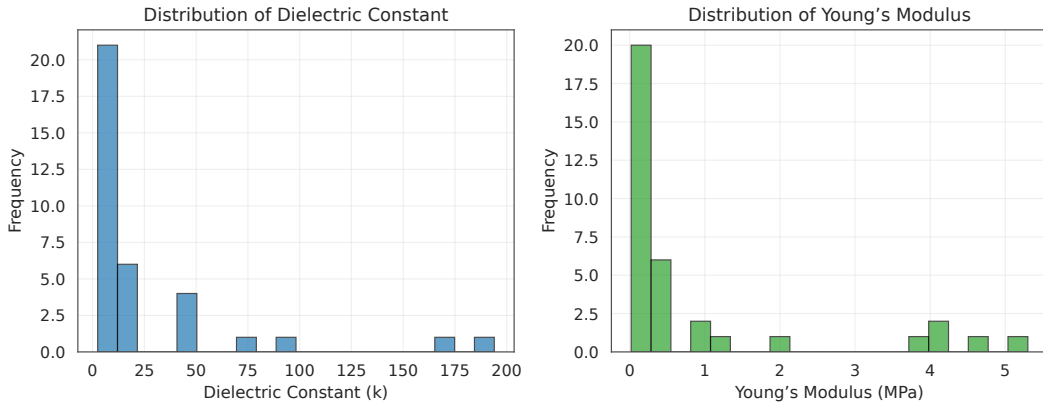


Figure 1: Distributions of dielectric constant (k) and Young’s modulus (E) across all curated acrylate-based dielectric elastomers. Most samples exhibit moderate-to-low dielectric constant and low modulus, with very few high- k outliers indicating enhanced polarization mechanisms.

4 Methodology

This section outlines the overall learning framework for data-efficient prediction of elastomer properties. As illustrated in Figure 2, our approach processes two complementary modalities, sequence-based and graph-based polymer representations, using their respective pretrained encoders. We explore two fusion strategies for integrating these modality-specific embeddings: a late fusion approach, where each modality produces an independent prediction that is subsequently combined, and a latent-space aligned early fusion approach, where lightweight projection heads first map the embeddings into a shared representation before fusion.

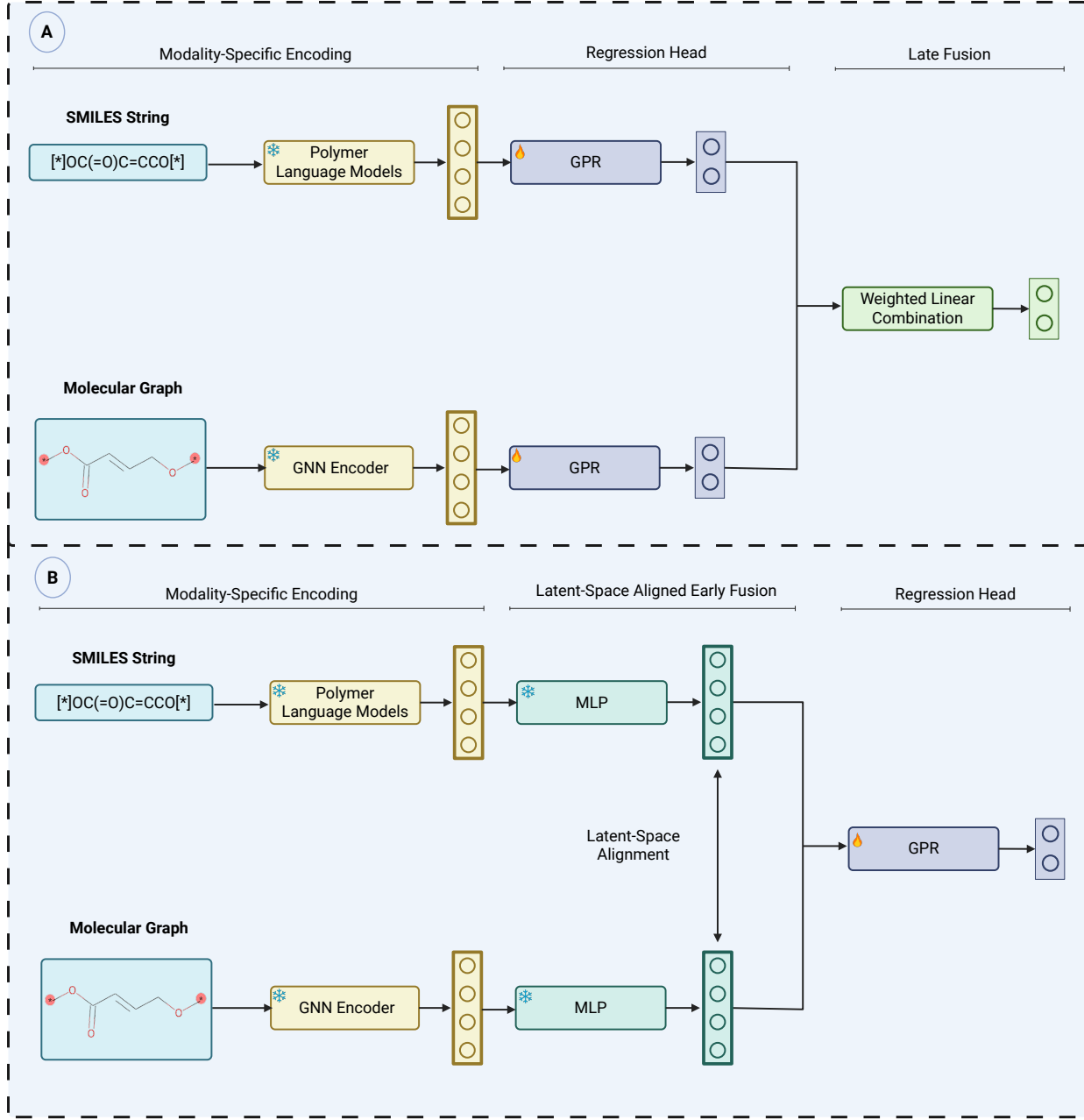


Figure 2: Overview of the proposed multimodal learning framework for elastomer property prediction. **(A) Late-fusion:** sequence-based and graph-based polymer representations are obtained from pretrained Polymer Language Models and a pretrained GNN encoder, respectively. Each embedding is passed through a Gaussian Process Regressor (GPR), and the final prediction is obtained via a weighted linear combination of the two modality-specific outputs. **(B) Latent-space aligned early fusion:** pretrained encoders first generate modality-specific embeddings, which are mapped into a shared representation space using lightweight MLP projection heads trained via latent-space alignment. The aligned embeddings are fused and subsequently passed to a shared GPR for joint prediction of dielectric constant and Young’s modulus.

4.1 Pretrained Sequence-Based Embeddings

For the sequence modality, we employ pretrained Transformer-based polymer language models to extract sequence-level representations from polymer SMILES strings. Instead of conducting pretraining from scratch, we leverage existing state-of-the-art models in the field, such as PolyBERT¹² and TransPolymer,¹⁴ which have been trained on large-scale, unlabeled polymer corpora using self-supervised objectives like masked-token prediction. These models capture the chemical syntax and substructural regularities inherent to polymer chains, enabling effective transfer of domain knowledge to downstream tasks. For each polymer, we obtain a fixed-length embedding vector by applying mean pooling across token embeddings, yielding a compact representation that encodes both chemical and contextual information relevant to dielectric and mechanical properties.

4.2 Pretrained Graph-Based Embeddings

To complement the sequence modality, we pretrain a graph-based encoder that captures the topological and structural characteristics of polymers. Each polymer is represented as a molecular graph, where atoms correspond to nodes and chemical bonds correspond to edges. Node features are defined by atomic numbers, and edge features encode bond types (single, double, triple, aromatic). Graphs are constructed from standardized SMILES strings using RDKit, ensuring consistency with the sequence-based representations.

The graph encoder is built upon the Graph Isomorphism Network (GIN)⁴¹ architecture, a message-passing neural network designed to effectively capture the structural and chemical information of molecular graphs. Each polymer is represented as a graph where atoms correspond to nodes and chemical bonds correspond to edges, with node features defined by atomic numbers and edge features by bond types (single, double, triple, aromatic). The encoder is trained in a self-supervised manner using two complementary objectives: (i) *masked-atom prediction*, in which a random subset of atom tokens is masked and recovered from their graph context, and (ii) *bond-type prediction*, which encourages the model to infer the chemical bond category between connected atoms. This dual self-supervised objective enables the encoder to learn transferable representations

that capture both local chemical environments and global structural dependencies without relying on labeled data.

Pretraining is performed on the PI1M database,⁴² which contains approximately one million unique polymers curated to support machine learning research in polymer informatics. After pre-training, each polymer graph is encoded into a fixed-length latent vector through a global pooling operation, yielding embeddings that encapsulate the polymer’s topological and electronic characteristics. These pretrained graph representations provide complementary structural information to the language-based embeddings and serve as one modality in our multimodal fusion framework for downstream property prediction.

4.3 Fusion Strategy

We explore two complementary fusion strategies for integrating information from the sequence and graph modalities: early fusion and late fusion.

4.3.1 Early Fusion

In this approach, the embeddings generated by the pretrained sequence and graph encoders are combined before regression. We evaluate both naive variants, such as feature concatenation and element-wise averaging, and aligned early-fusion variants, where each modality is first projected into a shared latent space using lightweight MLP heads trained with a CLIP-style contrastive objective.⁴³ This alignment step encourages the two embedding spaces to become semantically consistent, enabling more meaningful feature-level integration. The fused representation is then passed to a single regression head to predict the dielectric constant jointly and Young’s modulus.

4.3.2 Late Fusion

In contrast, late fusion combines information at the prediction level rather than at the feature level. Each modality is first processed independently through a regression pipeline to predict dielectric constant and Young’s modulus. The final prediction \hat{y} is obtained by combining the outputs from

the sequence-based branch (\hat{y}_{seq}) and the graph-based branch (\hat{y}_{graph}) using a weighted linear combination:

$$\hat{y} = \alpha \hat{y}_{\text{seq}} + (1 - \alpha) \hat{y}_{\text{graph}},$$

where $\alpha \in [0, 1]$ controls the relative contribution of each modality. The optimal α is determined via grid search to maximize the mean coefficient of determination (R^2) across both target properties. This late-fusion approach allows the framework to balance complementary information from structural and chemical representations while maintaining robustness in the low-data regime.

4.4 Regression Head

For downstream property prediction, we employ a multi-output Gaussian Process Regressor (GPR)⁴⁴ as the regression head. The GPR is a non-parametric Bayesian model that is particularly well suited for small datasets, as it does not rely on extensive parameterization and naturally incorporates uncertainty estimation. In our framework, we hypothesize that the embeddings extracted from pretrained sequence and graph encoders already contain rich and informative representations of polymer structure and chemistry. Therefore, a deep neural network is unnecessary for further feature extraction; instead, the GPR serves as a lightweight, data-efficient predictor that maps the pretrained embeddings to target properties.

5 Experiments

5.1 Experimental Setup

All experiments are conducted under an extreme data-scarcity setting to evaluate the robustness of the proposed multimodal learning framework. We adopt a Leave-One-Out Cross-Validation (LOOCV) protocol, in which a single elastomer sample is held out for testing while the remaining samples are used for training. This process is repeated until every sample has served as the test case once, ensuring unbiased evaluation despite the small dataset size.

During training, both the pretrained sequence and graph encoders remain frozen to preserve the structural and chemical knowledge acquired from large-scale polymer corpora. The embeddings produced by each encoder are processed through a lightweight regression pipeline consisting of feature standardization, dimensionality reduction via Principal Component Analysis (PCA), and a multi-output GPR that jointly predicts dielectric constant and Young’s modulus. This setup enables reliable learning in the small-data regime and allows fair comparison across all baseline and multimodal configurations evaluated in this study.

Model performance is evaluated using two complementary metrics: the coefficient of determination (R^2) and the root mean squared error (RMSE). The R^2 metric measures the proportion of variance in the target property that is explained by the model, with higher values indicating stronger predictive performance; it is reported separately for the dielectric constant (k) and Young’s modulus (E). RMSE quantifies the average magnitude of prediction errors in the original units of each property, penalizing larger deviations more heavily and providing an interpretable measure of absolute prediction accuracy. For both metrics, we additionally report the mean value across the two targets to summarize overall model quality. All results correspond to averages over LOOCV folds, ensuring a robust and unbiased assessment of generalization under data-scarce conditions.

5.2 Baselines

Since we introduce a new dataset for soft high- k elastomers, we establish a comprehensive set of baselines to evaluate our framework and to quantify the contribution of each modeling component. All models use the same Gaussian Process Regressor (GPR) head to ensure consistency across comparisons.

We begin by evaluating unimodal models, using each modality independently. For the sequence modality, we compare several representation types, including traditional molecular descriptors such as Morgan fingerprints⁴⁵ generated from polymer SMILES using RDKit,⁴⁶ as well as pretrained polymer language models such as PolyBERT and TransPolymer. For the graph modality, we evaluate a pretrained GNN encoder. This unimodal analysis serves two key purposes: (i) it

establishes how well each modality performs on its own under extreme data scarcity, and (ii) it allows us to select the strongest sequence encoder and the strongest graph encoder to be used in our multimodal framework.

Next, after identifying the most effective unimodal representations, we evaluate our two multimodal integration strategies. Early fusion merges embeddings from both modalities before regression, whereas late fusion combines modality-specific predictions through a weighted linear combination. Comparing these fusion strategies allows us to characterize the trade-offs between joint representation learning and independent modality specialization in low-data settings.

Together, these baselines provide a structured hierarchy of comparisons, from classical descriptors to single-modality pretrained models, to our two multimodal fusion strategies, offering a comprehensive evaluation of the advantages introduced by pretrained multimodal learning for soft high- k elastomer property prediction.

5.3 Results and Discussion

Table 2 shows that pretrained representations consistently outperform traditional molecular descriptors in the unimodal setting, indicating that large-scale pretraining captures chemically meaningful patterns beyond handcrafted features like Morgan fingerprints. Among the sequence-based models, TransPolymer achieves the highest mean R^2 of 0.698, while the pretrained GIN graph encoder reaches 0.687, both substantially better than the Morgan fingerprint baseline at 0.581. These results underscore the value of learned molecular representations for modeling elastomer properties. However, unimodal models still fall short in fully capturing the complex structure–property relationships that govern both dielectric and mechanical behavior. In contrast, our multimodal framework achieves the best overall performance, with a mean R^2 of 0.758 and the lowest RMSE of 13.659 across targets. In addition to its superior accuracy, the multimodal model exhibits much lower variance across runs, indicating improved robustness and stability. These findings confirm that sequence- and graph-based representations offer complementary information, and that their integration yields more reliable and generalizable predictions, especially under data-scarcity con-

Table 2: Evaluation of unimodal and multimodal representations for elastomer property prediction.

Modality	Feature Representation	$R^2 \uparrow$			RMSE \downarrow		
		k	E	Mean	k	E	Mean
Sequence	Morgan Fingerprint	0.362 ± 0.043	0.800 ± 0.015	0.581 ± 0.023	34.070 ± 7.206	0.654 ± 0.142	17.362 ± 3.642
	PolyBERT (Pretrained)	0.459 ± 0.034	0.824 ± 0.017	0.641 ± 0.019	31.150 ± 7.797	0.601 ± 0.185	15.875 ± 3.953
	TransPolymer (Pretrained)	0.561 ± 0.035	0.835 ± 0.010	0.698 ± 0.019	28.336 ± 5.564	0.599 ± 0.089	14.467 ± 2.802
Graph	GIN Encoder (Pretrained)	0.528 ± 0.039	0.846 ± 0.010	0.687 ± 0.021	29.174 ± 6.600	0.581 ± 0.067	14.878 ± 3.303
Multimodal	Ours	0.624 ± 0.015	0.892 ± 0.020	0.758 ± 0.011	26.829 ± 0.526	0.489 ± 0.047	13.659 ± 0.258

ditions.

As shown in Table 3, the choice of fusion strategy has a substantial impact on predictive performance under extreme data scarcity. Naive early-fusion approaches, such as simple concatenation or element-wise averaging, yield limited improvements. Among them, averaging performs better than concatenation, achieving a mean R^2 of 0.646 and an RMSE of 15.996, but both remain suboptimal. These results indicate that directly merging heterogeneous sequence and graph embeddings without explicitly addressing cross-modal incompatibility can dilute task-relevant signals. Late fusion, which combines modality-specific predictions rather than representations, provides a more robust alternative. The weighted late-fusion strategy improves over naive early fusion, attaining a mean R^2 of 0.689 and an RMSE of 15.185. This suggests that allowing each modality to specialize independently before integration is beneficial in low-data settings, although performance remains constrained by the lack of explicit representation alignment. Incorporating latent-space alignment leads to the strongest results. Both aligned early-fusion variants outperform naive and late-fusion approaches by a clear margin. In particular, aligned element-wise averaging achieves the highest mean R^2 of 0.758 and the lowest RMSE of 13.659, while also exhibiting reduced variance across folds. This improvement is further illustrated in Figure 3, which visualizes the strong agreement between predicted and experimental values for both target properties under the best-performing configuration. These results demonstrate that aligning sequence and graph embeddings into a shared latent space prior to fusion is crucial for effective multimodal integration, enabling more accurate and stable prediction of elastomer properties under severe data scarcity.

Table 3: Evaluation of multimodal fusion strategies for elastomer property prediction.

Fusion Type	Method	$R^2 \uparrow$			$RMSE \downarrow$		
		k	E	Mean	k	E	Mean
Early Fusion	Concatenation	0.383 ± 0.109	0.701 ± 0.106	0.542 ± 0.065	34.270 ± 2.873	0.809 ± 0.130	17.539 ± 1.421
	Averaging	0.481 ± 0.120	0.811 ± 0.061	0.646 ± 0.067	31.346 ± 3.390	0.645 ± 0.091	15.996 ± 1.696
Latent-Space Aligned Early Fusion	Concatenation	0.608 ± 0.014	0.895 ± 0.014	0.752 ± 0.012	27.386 ± 0.497	0.484 ± 0.032	13.935 ± 0.256
	Averaging	0.624 ± 0.015	0.892 ± 0.020	0.758 ± 0.011	26.829 ± 0.526	0.489 ± 0.047	13.659 ± 0.258
Late Fusion	Weighted Prediction ($\alpha = 0.3$)	0.537 ± 0.015	0.841 ± 0.020	0.689 ± 0.012	29.775 ± 0.478	0.595 ± 0.034	15.185 ± 0.238

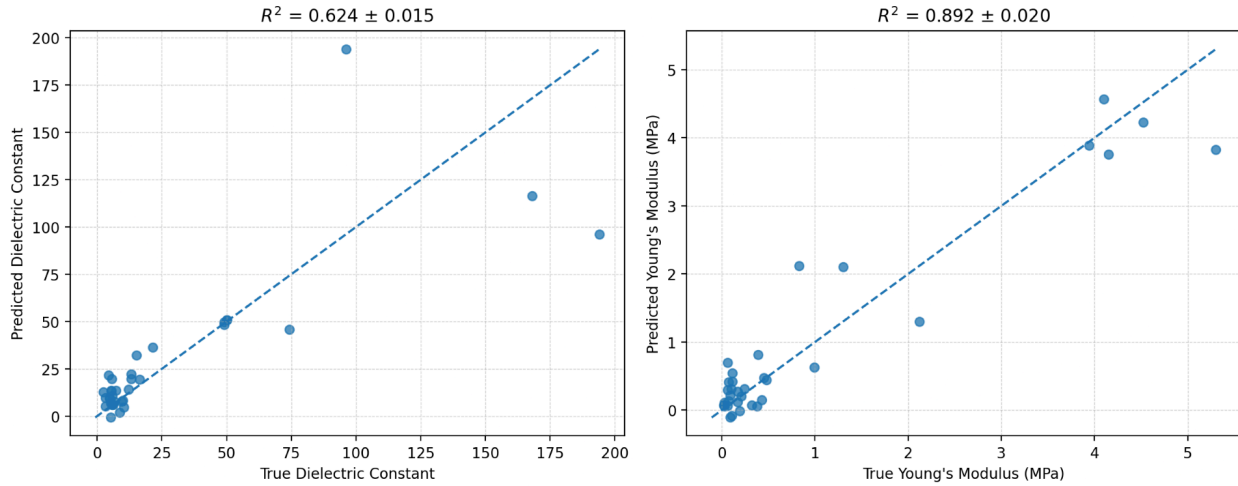


Figure 3: Correlation between predicted and experimental values for the two target properties using the best-performing multimodal configuration, namely latent-space aligned early fusion with element-wise averaging.

6 Conclusion

In this work, we addressed the challenge of predicting the dielectric and mechanical properties of soft high- k dielectric elastomers from molecular sequences under extreme data scarcity conditions. For this purpose, we first curated a high-quality dataset based on soft acrylate-based dielectric elastomers from peer-reviewed literature, where experimentally measured dielectric constants and Young’s moduli, along with molecular sequences, are consolidated into a consistent machine-readable format. Building on this dataset, we introduced a multimodal learning framework that integrates pretrained sequence-based and graph-based polymer representations. By transferring chemical and structural knowledge learned from existing large polymer corpora, the framework captured complementary information that cannot be reliably extracted from the small target dataset alone. Among the fusion strategies evaluated, latent-space aligned early fusion proved most ef-

fective, consistently outperforming unimodal models and naive fusion schemes. These findings emphasize the importance of cross-modal representation alignment and demonstrate that well-designed multimodal integration substantially improves learning robustness with limited data.

Moving forward, our work may open up numerous opportunities from polymer informatics to materials innovation. First, despite its relatively small size, our curated dataset of acrylate-based dielectric elastomers represents the first example that couples dielectric and mechanical properties for emerging soft and stretchable polymers. Similar data curation protocols and learning pipelines can be applied to expand the current dataset to incorporate other elastomer backbone systems such as silicones and urethanes. Second, beyond the linear molecular sequences used in this study, additional quantitative structural information from experimental characterization (e.g., NMR) or computational simulations can be incorporated into a modified learning framework to correlate intra- and inter-chain interactions with the resulting dielectric and mechanical properties. Third, this study mainly focuses on pure polymer-based elastomers; meanwhile, considerable efforts have been done to optimizing dielectric performance through the incorporation of extrinsic dopants into elastomer matrices. Continued work is needed to expand the dataset with more complex composites and accurately capture the effects of dopant-elastomer interactions. Fourth, by integrating property prediction and formulation suggestion within our model, these capabilities can be experimentally validated and used to guide high-throughput polymer synthesis, thus accelerating the closed-loop, iterative development of soft high- k dielectric elastomers.

7 Data Availability

The curated dataset and all source code used in this study will be publicly available in our GitHub repository at <https://github.com/HySonLab/Polymers>.

References

- (1) Amamoto, Y. Data-driven approaches for structure–property relationships in polymer science for prediction and understanding. *Polymer Journal* **2022**, *54*, 957–967.
- (2) Doan Tran, H.; Kim, C.; Chen, L.; Chandrasekaran, A.; Batra, R.; Venkatram, S.; Kamal, D.; Lightstone, J. P.; Gurnani, R.; Shetty, P.; others Machine-learning predictions of polymer properties with Polymer Genome. *Journal of Applied Physics* **2020**, *128*.
- (3) Bicerano, J. *Prediction of polymer properties*; cRc Press, 2002.
- (4) Yu, X.; Wang, X.; Li, X.; Gao, J.; Wang, H. Prediction of glass transition temperatures for polystyrenes by a four-descriptors QSPR model. *Macromolecular theory and simulations* **2006**, *15*, 94–99.
- (5) Le, T.; Epa, V. C.; Burden, F. R.; Winkler, D. A. Quantitative structure–property relationship modeling of diverse materials properties. *Chemical reviews* **2012**, *112*, 2889–2919.
- (6) Rahman, A.; Deshpande, P.; Radue, M. S.; Odegard, G. M.; Gowtham, S.; Ghosh, S.; Spear, A. D. A machine learning framework for predicting the shear strength of carbon nanotube–polymer interfaces based on molecular dynamics simulation data. *Composites Science and Technology* **2021**, *207*, 108627.
- (7) Simine, L.; Allen, T. C.; Rossky, P. J. Predicting optical spectra for optoelectronic polymers using coarse-grained models and recurrent neural networks. *Proceedings of the National Academy of Sciences* **2020**, *117*, 13945–13948.
- (8) Webb, M. A.; Jackson, N. E.; Gil, P. S.; de Pablo, J. J. Targeted sequence design within the coarse-grained polymer genome. *Science advances* **2020**, *6*, eabc6216.
- (9) Weininger, D. SMILES, a chemical language and information system. 1. Introduction to methodology and encoding rules. *Journal of chemical information and computer sciences* **1988**, *28*, 31–36.

(10) Daylight Theory: SMARTS - A Language for Describing Molecular Patterns — daylight.com. <https://www.daylight.com/dayhtml/doc/theory/theory.smarts.html>, [Accessed 05-11-2025].

(11) Krenn, M.; Häse, F.; Nigam, A.; Friederich, P.; Aspuru-Guzik, A. Self-referencing embedded strings (SELFIES): A 100% robust molecular string representation. *Machine Learning: Science and Technology* **2020**, *1*, 045024.

(12) Kuenneth, C.; Ramprasad, R. polyBERT: a chemical language model to enable fully machine-driven ultrafast polymer informatics. *Nature communications* **2023**, *14*, 4099.

(13) Xu, C.; Wang, Y.; Barati Farimani, A. TransPolymer: a Transformer-based language model for polymer property predictions. *npj Computational Materials* **2023**, *9*, 64.

(14) Wang, F.; Guo, W.; Cheng, M.; Yuan, S.; Xu, H.; Gao, Z. Mmpolymer: A multimodal multitask pretraining framework for polymer property prediction. Proceedings of the 33rd ACM International Conference on Information and Knowledge Management. 2024; pp 2336–2346.

(15) Huang, Q.; Li, Y.; Zhu, L.; Zhao, Q.; Yu, W. Unified multimodal multidomain polymer representation for property prediction. *npj Computational Materials* **2025**, *11*, 153.

(16) Feng, W.; Sun, L.; Jin, Z.; Chen, L.; Liu, Y.; Xu, H.; Wang, C. A large-strain and ultrahigh energy density dielectric elastomer for fast moving soft robot. *Nature Communications* **2024**, *15*, 4222.

(17) Yin, L.-J.; Du, B.; Hu, H.-Y.; Dong, W.-Z.; Zhao, Y.; Zhang, Z.; Zhao, H.; Zhong, S.-L.; Yi, C.; Qu, L.; Dang, Z.-M. A high-response-frequency bimodal network polyacrylate elastomer with ultrahigh power density under low electric field. *Nature Communications* **2024**, *15*, 9819.

(18) Han, Z.; Peng, Z.; Guo, Y.; Wang, H.; Plamthottam, R.; Pei, Q. Hybrid Fabrication of

Prestrain-Locked Acrylic Dielectric Elastomer Thin Films and Multilayer Stacks. *Macromolecular Rapid Communications* **2023**, *44*, e2300160.

- (19) Shi, Y.; Askounis, E.; Plamthottam, R.; Libby, T.; Peng, Z.; Youssef, K.; Pu, J.; Pelrine, R.; Pei, Q. A processable, high-performance dielectric elastomer and multilayering process. *Science* **2022**, *377*, 228–232.
- (20) Zhao, Y.; Feng, Q.-Y.; Xie, Y.-K.; Zhang, Z.-L.; Yin, L.-J.; Dang, Z.-M. Advanced Acrylate Dielectric Elastomers with Large Actuation Strains at Very Low Electric Field. *ACS Applied Polymer Materials* **2022**, *4*, 8892–8899.
- (21) Yin, L.-J.; Zhao, Y.; Zhu, J.; Yang, M.; Zhao, H.; Pei, J.-Y.; Zhong, S.-L.; Dang, Z.-M. Soft, tough, and fast polyacrylate dielectric elastomer for non-magnetic motor. *Nature Communications* **2021**, *12*, 4517.
- (22) Xiong, L.; Li, D.; Yang, Y.; Ye, X.; Huang, Y.; Xu, E.; Xia, C.; Yang, M.; Liu, Z.; Cui, X.; Wang, F.; Huang, Y. Tailoring crosslinking networks to fabricate photocurable polyurethane acrylate (PUA) dielectric elastomer with balanced electromechanical performance. *Reactive and Functional Polymers* **2023**, *183*, 105498.
- (23) Ha, S. M.; Park, I. S.; Wissler, M.; Pelrine, R.; Stanford, S.; Kim, K. J.; Kovacs, G.; Pei, Q. High electromechanical performance of electroelastomers based on interpenetrating polymer networks. *Electroactive Polymer Actuators and Devices (EAPAD)* 2008. Bellingham, WA, 2008; p 69272C, Held 10–13 March 2008, San Diego, California, USA.
- (24) Liu, L.; Zhang, K.; Liu, J.; Zhu, L.; Xie, R.; Lv, S. Significant improvements in the electromechanical performance of dielectric elastomers by introducing ternary dipolar groups. *Reactive and Functional Polymers* **2022**, *172*, 105177.
- (25) Tan, M. W. M.; Thangavel, G.; Lee, P. S. Enhancing dynamic actuation performance of dielectric elastomer actuators by tuning viscoelastic effects with polar crosslinking. *NPG Asia Materials* **2019**, *11*, 62, Published: 25 Oct 2019.

(26) Shao, J.; Wang, J.-W.; Wei, L.; Wu, S.-Q.; Yang, Y.-H.; Ren, H. A novel high dielectric constant acrylic resin elastomer nanocomposite with pendant oligoanilines. *Composites Part B: Engineering* **2019**, *176*, 107216, Available online 23 July 2019.

(27) Gao, X.-H.; Wang, J.-W.; Liu, D.-N.; Wang, X.-Z.; Wang, H.-Q.; Wei, L.; Ren, H. Improving the dielectric properties of acrylic resin elastomer with reduced graphene oxide decorated with polystyrene. *European Polymer Journal* **2021**, *150*, 110418.

(28) Han, Z.; Peng, Z.; Guo, Y.; Wang, H.; Plamthottam, R.; Pei, Q. Hybrid Fabrication of Prestrain-Locked Acrylic Dielectric Elastomer Thin Films and Multilayer Stacks. *Macromolecular Rapid Communications* **2023**, *44*, e2300160.

(29) Zhao, Y.; others Remarkable electrically actuation performance in advanced acrylic-based dielectric elastomers without pre-strain at very low driving electric field. *Polymer* **2018**, *137*, 269–275.

(30) Chen, Z. Ultrasoft-yet-strong pentablock copolymer for dielectric elastomer. *Chemical Engineering Journal* **2021**, *405*, 126634.

(31) Sung, G.; Yu, C.; Park, J.-M.; Lee, Y. H.; Park, C. S.; Lee, H.; Kwon, M. S.; Sun, J.-Y. High-k zwitterionic dielectric elastomers with internal plasticization for low-voltage actuation. *Materials Today* **2025**, *88*, 109–116.

(32) Ankit; Tiwari, N.; Ho, F.; Krisnadi, F.; Kulkarni, M. R.; Nguyen, L. L.; Koh, S. J. A.; Mathews, N. High-k, Ultrastretchable Self-Enclosed Ionic Liquid-Elastomer Composites for Soft Robotics and Flexible Electronics. *ACS Applied Materials & Interfaces* **2020**, *12*, 37561–37570.

(33) Li, Y.; Zhao, Q.; Huang, J.; Hu, X.; Yan, Y.; Li, L. Significant Improvements in the Dielectric Performance of Dielectric Elastomers with Polar Cyano Groups. SSRN, 2024; <https://ssrn.com/abstract=5031777>, SSRN working paper. Posted: 2024-11-23.

(34) Wang, H.; Tan, M. W. M.; Poh, W. C.; Gao, D.; Wu, W.; Lee, P. S. A highly stretchable, self-healable, transparent and solid-state poly(ionic liquid) filler for high-performance dielectric elastomer actuators. *Journal of Materials Chemistry A* **2023**, *11*, 14159–14168.

(35) Adeli, Y.; Venkatesan, T. R.; Mezzenga, R.; Nüesch, F. A.; Opris, D. M. Synthesis of Bottlebrush Polymers with Spontaneous Self-Assembly for Dielectric Generators. *ACS Applied Polymer Materials* **2024**, *6*, 4999–5010.

(36) Park, J.-M.; Park, C. S.; Kwak, S. K.; Sun, J.-Y. Glass transition temperature as a unified parameter to design self-healable elastomers. *Science Advances* **2024**, *10*, eadp0729.

(37) Zhang, Q.; Yu, W.; Zhao, J.; Meng, C.; Guo, S. A Review of the Applications and Challenges of Dielectric Elastomer Actuators in Soft Robotics. *Machines* **2025**, *13*, 101.

(38) Liu, L.; Zhang, K.; Liu, J.; Zhu, L.; Xie, R.; Lv, S. Significant improvements in the electromechanical performance of dielectric elastomers by introducing ternary dipolar groups. *Reactive and Functional Polymers* **2022**, *172*, 105177.

(39) Shi, L.; Yang, R.; Lu, S.; Jia, K.; Xiao, C.; Lu, T.; Wang, T.; Wei, W.; Tan, H.; Ding, S. Dielectric gels with ultra-high dielectric constant, low elastic modulus, and excellent transparency. *NPG Asia Materials* **2018**, *10*, 821–826.

(40) Bezsdudnov, I. V.; Khmelnitskaia, A. G.; Kalinina, A. A.; Ponomarenko, S. A. Dielectric elastomer actuators: materials and design. *Russian Chemical Reviews* **2023**, *92*, RCR5070.

(41) Xu, K.; Hu, W.; Leskovec, J.; Jegelka, S. How powerful are graph neural networks? *arXiv preprint arXiv:1810.00826* **2018**,

(42) Ma, R.; Luo, T. PI1M: a benchmark database for polymer informatics. *Journal of Chemical Information and Modeling* **2020**, *60*, 4684–4690.

(43) Radford, A.; Kim, J. W.; Hallacy, C.; Ramesh, A.; Goh, G.; Agarwal, S.; Sastry, G.;

Askell, A.; Mishkin, P.; Clark, J.; others Learning transferable visual models from natural language supervision. International conference on machine learning. 2021; pp 8748–8763.

(44) Williams, C.; Rasmussen, C. Gaussian processes for regression. *Advances in neural information processing systems* **1995**, 8.

(45) Morgan, H. L. The generation of a unique machine description for chemical structures-a technique developed at chemical abstracts service. *Journal of chemical documentation* **1965**, 5, 107–113.

(46) Rdkit: open-source cheminformatics <http://www.rdkit.org>.